ISSN 0915-633X

NATIONAL INSTITUTE FOR FUSION SCIENCE

A Global Simulation of the Magnetosphere with a Long Tail: Southward and Northward IMF

A. Usadi, A. Kageyama, K. Watanabe
and T. Sato

(Received – Jun. 6, 1991)

NIFS-99 Jun. 1991

RESEARCH REPORT
NIFS Series

NAGOYA, JAPAN

A Global Simulation of the Magnetosphere with a Long Tail: Southward and Northward IMF

A. Usadi and A. Kageyama,
Faculty of Science, Hiroshima University, Japan
K. Watanabe and T. Sato
National Institute for Fusion Science, Nagoya, Japan

Abstract

Through a global three dimensional MHD simulation, the effect of the Interplanetary Magnetic Field (IMF), both northward and southward, on Earth's magnetosphere has been investigated. A southward IMF, upon reconnecting at the dayside magnetopause of the Earth's magnetic field is swept back by solar wind flow and drapes the magnetotail. This gives rise to a plasma sheet cross-tail current increase and explosive magnetic reconnection at around $15R_E$. This reconnection results in the formation of a large plasmoid which grows much faster than for the simulation with no IMF, thus supporting, in a convincing way with a minimum of assumptions, previous notions that a southward IMF is a driving mechanism of plasma sheet reconnection. A northward IMF is observed to reconnect with the magnetosphere along the cusp shoulder, stripping magnetic field lines away and weakening compression of the plasma sheet. In order to accomodate a balance of magnetic to dynamic pressure along the magnetopause, the magnetosphere changes from its usual comet-like shape to that resembling a tadpole as it attempts to return to a dipolar structure. Plasmasheet reconnection is inhibited.

Keywords; *computer simulation, magnetohydrodynamics, magnetosphere, magnetotail, plasmoid, magnetic reconnection, plasma sheet, interplanetaly magnetic field, magnetospheric substorm*

Introduction

Since Kristian Birkland discovered, in the beginning of the 20th century, that currents were flowing in the ionosphere during aurora displays, understanding the complex interactions of Earth's magnetic field, ionosphere, and solar forces has been a tantalizing problem. Answers to old questions have led to new and more difficult puzzles which require a highly non-linear analysis only large scale, global computer simulations can provide. Global phenomena such as the reaction time of the magnetosphere to the changing solar wind and the origin of magnetosphere substorms cannot be explained by the results of local simulations.

Satellite and Earth based observations of magnetosphere and Interplanetary Magnetic Field activity lead us to believe that there is a heavy dependence between substorm activity and the IMF. In particular, the southward component of the IMF seems to trigger at least some magnetosphere substorms.

There are a number of theories which attempt to explain the mechanisms of magnetosphere substorms which include the sudden and simultaneous injection of energy into the ionosphere and out towards the tail. Among them, the near-Earth neutral line model[*Hones*, 1979] or some modification[e.g., *Liu*, 1991] seems most viable. Recent papers [*Slaven et al.*, 1989; *Richardson et al.*, 1989; *Kettmann et al.*, 1990] presenting detailed analysis of ISEE 1 and ISEE 2 data have provided strong evidence that near-Earth reconnection and plasmoid formation are indeed taking place and are directly controlled by the southward/northward component of the IMF.

The concept of magnetic reconnection occuring between the IMF and magnetosphere was introduced by Dungey [1961]. Due to reconnection between a southward IMF and geomagnetic field at the dayside magnetopause, energy is transferred to the magnetosphere. Due to reconnection in the plasma sheet, energy contained in the magnetosphere is thought to be transfered partly to the ionosphere and partly back to the solar wind. And due to reconnection between a northward IMF and geomagnetic field at the shoulder of the magnetosphere cusp, energy is thought to be stripped away from the magnetosphere.

The purpose of this research is to clarify the role of the southward and northward components of the IMF in its interaction with the magnetosphere. In particular, we sought to answer the following 2 questions.

- What are the large scale changes in magnetosphere behavior due to exposure to a solar wind with a southward or northward magnetic field?
- How do the southward and northward components of the IMF control plasma sheet reconnection processes?

Model

Important characteristics of the model and code used, which have been explained in detail previously [*Watanabe and Sato*, 1990, *Kageyama et al.*, 1991], are be briefly reviewed here.

The initial magnetic field configuration was comprised of the superposition of Earth's point dipole field and its image dipole outside and in front of the simulation region. This box was filled with a plasma such that its density was determined by a constant initial Alfvén velocity of $700 km/s$ and the magnetic field. The position of the polar cusp was shown to be independent of the position of the initial image dipole.

The simulation was performed over the region

Dawn-Dusk axis	$0 \leq X \leq 50 R_E$	70 grid points
Sun-Earth axis	$-95 R_E \leq Y \leq 30 R_E$	187 grid points
Earth Polar axis	$0 \leq Z \leq 50 R_E$	70 grid points

using an exponentially stretched grid mesh such that near the Earth, where abrupt changes in physical quantities merited a finer mesh, the grid spacing was approximately $0.5 R_E$ in all directions. Farther down towards the tail boundary, where longer wavelength phenomena dominate, the grid spacing was increased to $1.2 R_E$. This was done in order to accomodate as large a region as possible while maintaining numerical credibility. The front boundary was extended from $20 R_E$ [*Kageyama et al.*, 1991] to $30 R_E$ in order to move boundary effects away from the magnetosphere. In doing so, the need for a front numerical damping region, as described by Kageyama et al., disappeared. The only numerical damping region used was that to quiet transient flows during magnetosphere formation since our interest was not in the formation itself. This damping region was removed gradually by $t \approx 2.2 hours$, much sooner than the simulation of Kageyama et al., with no ill effects.

The simulation region defines only one quarter of the magnetosphere. The interest of this work centers on the affects of the southward/northward component of the IMF on the magnetosphere. With no dawn-dusk component of B in the IMF, the physical problem becomes symmetrical or anti-symmetrical across the equatorial and meridian planes.

The debate over the adequacy of the MHD approximation to describe the global behavior of the magnetosphere has been nicely summarized in several places [e.g., *Hasegawa and Sato*, 1989, *Lui*, 1986, *Coroniti*, 1986]. Its validity here is based on the following. We are interested in the IMF and it's affect on the magnetosphere and plasmoid formation. These processes typically occur on the order of minutes to hours over a scale length of $1 \sim 100 R_E$ where $1 R_E \equiv 6370 km$. Consider the environs of the Earth/solar wind interaction region where the magnetic field intensity is on the order of $10^{-9} \sim 10^{-8} Tesla$, the solar wind ion temperature is on the order of kev, and electron temperature is on the order of $100 ev$. From this, we know that the ion gyroradius $\approx 500 km$ and electron gyroradius $\approx 50 km$. In addition, the ion and electron cyclotron frequencies are, approximately $10^{-1} sec^{-1}$ and $10^{2} sec^{-1}$, respectively. Thus, if we are careful to limit what we may say about the results of the simulation the MHD approximation seems quite suitable to describe global magnetosphere substorm activity and is certainly the only method viable with today's computers. We thus proceed to write the resistive MHD equations:

$$\frac{\partial \rho}{\partial t} = -\nabla \cdot (\rho \mathbf{v}) \tag{1}$$

$$\rho \frac{d\mathbf{v}}{dt} = -\nabla p + \mathbf{j} \times \mathbf{B} \tag{2}$$

$$\frac{\partial \mathbf{B}}{\partial t} = -\nabla \times \mathbf{E} \tag{3}$$

$$\frac{dp}{dt} = -\gamma\, p \nabla \cdot \mathbf{v} + \frac{1}{\sigma}(\gamma - 1)\mathbf{j}^2 \tag{4}$$

$$\mathbf{E} = \frac{1}{\sigma}\mathbf{j} - \mathbf{v} \times \mathbf{B} \tag{5}$$

$$\mathbf{j} = \frac{1}{\mu_0} \nabla \times \mathbf{B} \tag{6}$$

where $\mathbf{B}, \mathbf{E}, \mathbf{v}, p, \rho$, and $\mathbf{j}$ are the total magnetic field, electric field, plasma flow velocity, plasma kinetic pressure, plasma mass density, and current density, respectively. In addition, μ_0 is the permeability of a vacuuum and γ is the adiabatic constant.

The resistivity of the system in question and, in particular, of the plasma sheet is

not quantitatively known. It is probably rather small over most regions and is usually neglible since the density of particles in space plasmas is low. Simulation runs including the resistive terms were made and it was found that reconnection rates at the dayside, cusp shoulder, and plasma sheet are independent of resistivity (at least until a minimum equal to the numerical resistivity). This agrees well with previous work concerning a finite resistivity[*Sato and Hayashi*, 1979], which showed that magnetic reconnection rates are only slightly dependent on resistivity provided it's not equal to zero. Kageyama et al. [1991] performed several runs of their simulation with no IMF in order to determine the minimum $\eta \equiv \frac{1}{\mu_0 \sigma}$ which begins to noticeably affect the simulation results. In doing so, they were able to roughly estimate the value of the numerical resistivity $\eta \approx 5 \times 10^{-4}$. For the results presented here, the resitive terms were not calculated; the small numerical resistivity was sufficient.

These MHD equations were solved using a high precision code developed by Sato and others [*Watanabe and Sato*, 1990] which advances the physical quantities in time using a fourth order Runge-Kutta-Gill method and second order centered-difference method in space. The time step used was $\approx$ 3 seconds so that phenomena on the order of hours could be analyzed.

How should one integrate the ionosphere and magnetosphere? The ionosphere is highly collisional and is only partially ionized. The single fluid description does not sufficiently describe ionosphere behavior. Plasma can flow perpendicular to magnetic field lines there under the influence of electric fields. Thus current flowing down along magnetic field lines from the magnetosphere can close a circuit with currents flowing up in other regions. This phenomenon has been well studied previously [e.g., *Watanabe et al.*, 1989]. Most importantly, however, the typical scale lengths are orders of magnitude smaller than those in the magnetosphere. Thus, the ionosphere was modeled as a resistive shell with physical quantities being damped in the region from 8Re to 5Re. The damping method approximately mimics the height integrated ionospheric resitivity[*Watanabe et al.*, 1989]. A proper model of the ionosphere and magnetosphere simultaneously must await the next generation of computers.

A solar wind flow with no IMF was introduced at the sunward boundary so that by $t \approx 10$ minutes it reached a steady state where $v = 300km/s$, $\rho = 5 \cdot m_H/cm^3$, and $T = 20ev$. The solar wind flowed from the sunward boundary to the tail boundary in about one hour.

The formation process of a magnetosphere with a long tail and magnetically neu-

tral plasma sheet takes approximately one hour and was well described by Kageyama et al. [1991]. The major characteristics include the existence of a bow shock in front of the dayside magnetopause located at $13R_E$ and $11R_E$, respectively. A polar, magnetic cusp forms slightly forward of the magnetic pole towards the sun. A hot plasma sheet behind the Earth in the tail forms and maintains a temperature $\approx 0.5kev$ (Figure 1-B).

The shape of the magnetosphere is produced and maintained by the current flowing along the surface of the magnetosphere, also called the Chapman-Ferraro current. In addition, a dawn-to-dusk diamagnetic current flows in the plasma sheet and closes with the Chapman-Ferraro current. Current vectors on the equatorial cross section of the just formed magnetosphere reveal the presence of both in Figure 1-A.

Once the magnetosphere formation is nearly complete($t = 1hour$), a northward or southward IMF was introduced at the sunward boundary such that its strength reaches 5nT within 10 minutes. Three separate cases involving an IMF were simulated once the magnetosphere was formed.

1. A solar wind containing a southward IMF blowing continuously for 2 hours.

2. A solar wind containing a northward IMF blowing continuously for 2 hours.

3. A solar wind containing a southward IMF blowing for 1 hour. Subsequently,the IMF is changed to a northward IMF and is allowed to blow for 1 hour.

Results

Southward IMF – The IMF contained in the solar wind arrives at the surface of the dayside magnetopause 10 minutes later at about 1.2hours. Figure 2 shows the changes in structure of the magnetosphere over a 1.5 hour period. Magnetosphere and IMF field lines and solar wind flow lines are drawn. In addition, the plasmoid produced through magnetic reconnection occurring in the plasma sheet is drawn by dotted lines.

When a southward magnetic field imbedded in the solar wind is forced against the oppositely directed field lines of the dayside magnetopause diffusion of the magnetic fields occurs in the presence of the Chapman-Ferraro current and resistivity. The IMF then reconnects with the geomagnetic field lines at the surface of the dayside magnetopause along the equatorial plane. The plasma flow pushes these reconnected

field lines tailward and eventually drapes them over the tail region, thus adding to the magnetic flux of the magnetotail lobes. Note that this is contrary to some simulation results that report multiple dayside reconnection. In the results of *Shi et al.* [1988], no bow shock exists in front of the magnetopause. The solar wind which impinges upon the magnetopause, therefore remains super sonic and super Alfvénic. This leads to an unrealistic current distribution on the dayside magnetopause and, therefore, reconnection at latitudes above the equatorial plane. Multiple reconnection may still occur, but on a large scale, dayside reconnection seems to be localized around the equatorial plane.

Reconnection at the dayside magnetopause is linked to processes in the magnetosphere in several ways. First, the reconnected field lines which drape the tail add magnetic flux to the lobes and result in the increase of forces which adiabatically compress the plasma sheet. Hence, the plasma sheet temperature rises. In addition, the diamagnetic, cross-tail current is increased. Thus, plasma sheet reconnection rates, which are directly related to the magnitude of the cross-tail current, and associated phenomena are greatly enhanced.

From about 1.1 to 1.5 hours, the hot plasma sheet thins as the magnetic field decreases. It thus becomes more magnetically neutral. Looking at Figure 5-A, we see at $t \approx 2.1 hours$ that the cross-tail current peaks between $x = -14R_E$ and $-18R_E$. The pressure peaks slightly closer to the Earth at about $-9R_E$, but remains high until $-20R_E$. The temperature approaches a value of $0.6 \sim 0.7 kev$.

Reconnection at the plasma sheet between the northern lobe field lines and oppositely directed southern lobe field lines begins sometime between 1.5 and 1.6 hours. This is approximately 20 minutes after the southward IMF begins to reconnect with dayside geomagnetic field lines [*Baker et al.*, 1983]. Plasmoid expansion is immediate as it is ejected tailward under pressure exerted by the lobes.

As dayside reconnection continues, the magnetic flux of the dayside magnetosphere decreases. The lost magnetic flux has been pulled back and added to the magnetic lobes. The dayside magnetosphere is said to be 'eroded' by reconnecting with a southward IMF. Due to a decrease in the magnetic pressure force the location of the dayside magnetopause shifts one or two R_E towards the Earth.

Northward IMF – Reconnection at the shoulder of the polar cusp of $5nT$ northward IMF lines with geomagnetic field lines has been discussed before [e.g., *Ogino et al.*, 1985]. When a northward IMF impedes upon the magnetopause, solar

wind magnetic flux builds up on the dayside magnetopause. The Chapman-Ferraro current along the dayside magnetopause decreases dramatically due to an oppositely directed electric field (see Figure 5-B). As the IMF attempts to drape the magnetotail, the oppositely directed magnetic field lines of the Earth and IMF come into contact at the nothern and southern magnetosphere shoulders just above the cusps. As in the case for dayside reconnection, a small resistivity with the magnetosphere surface current leads to magnetic reconnection. In this case, however, the solar wind plasma flow blows part of the reconnected field line away, the part that is untied to the Earth. Thus, magnetic flux from the outer surface of the magnetotail lobes is pealed away like the skin of an onion (see Figure 3-A).

The effects of stripping off magnetic energy from the lobes of the magnetotail are several. As mentioned previously, when no IMF is present in the solar wind, the location of the magnetopause is determined by the balance of the magnetic pressure of the magnetosphere and the pressure of the solar wind. However, as the lobe flux is pealed away the magnetic pressure exerted along the magnetopause decreases, though the dynamic pressure exerted by the solar wind remains the same. The magnetotail transforms into a the shape of a 'tadpole' as it attempts to find a new equilibrium position for the magnetopause. In doing so, the plasma sheet is decompressed. The plasma sheet pressure drops and the cross tail current is decreased. Thus, reconnection processes are inhibited.

The speed of the transformation into the tadpole shape is apparently high. This may be due to the fact that the reconnection rate of the simulation is too high compared with the actual rate. Therefore, the actual rate of the change in magnetosphere shape may be slower than present results. But the tendency approaching a tadpole shape when the IMF continues to be northward is a reasonable result.

Southward→Northward IMF – In order to further reveal the behavior of the southward and northward solar magnetic fields as triggers of plasma sheet reconnection, the following simulation was also performed. For one hour, a southward IMF of $5nT$ in strength was exposed to the magnetosphere. In this time, plasma sheet reconnection and plasmoid expansion got well under way as can be seen in Figure 4-A. The southward IMF was turned off at the boundary and a northward IMF of the same strength was turned on immediately. As expected, the cross tail current was decreased (see Figure 6-I). The rate of reconnection decreased as evidenced by a decrease in the acceleration of plasma on either side of the neutral X line in the

plasma sheet (Figure 9 and Figure 6-I). In addition, the plasmoid ejection speed was slowed as seen in Figure 10.

A study of the magnetosphere with a long tail under the influence of a non-magnetized solar wind has been done before [*Kageyama et al.*, 1991]. It was necessary, however, to repeat the procedure using the new parameters developed for this research in order to discern effects due soley to a southward or northward IMF. In either case, very weak reconnection processes do begin some time between 1.5 and 1.6 hours. However, the plasmoid does not undergo an expansion phase until one hour later or $t = 2.5 hours$.

Discussion

These results strongly support the near earth, neutral line model of magnetosphere substorm activity. The addition of a southward IMF to the solar wind flow does indeed explosively drive plasma sheet reconnection. This is characteristic of driven reconnection. In addition, related processes such as plasmoid formation and plasma acceleration near the magnetically neutral line were very much dependent on the presence of a southward IMF.

For both the cases when a southward IMF is present and the case when no IMF is present, reconnection in the plasma sheet begins sometime between 1.5 and 1.6 hours. When no IMF is present, the reconnection is a weak process. In this case expansion of the plasmoid does not begin until about 2.5 hours and is slow. However, for the case when a southward IMF is present, the reconnection is explosive leading to immediate plasmoid expansion. This explosive reconnection and plasmoid expansion is clearly a direct result of the southward IMF.

Figure 6-I shows the change of pressure, temperature, and cross tail current at the point $14R_E$ behind the earth as a function of time. As can be seen, when a southward IMF is present in the solar wind, the pressure and cross tail current increase dramatically faster than for the case when no IMF is present. When no IMF is present, the plasma sheet temperature reaches a maximum of about $0.5 kev$. When a southward IMF is present, however, the temperature goes as high as $0.7 kev$. Similarly, the cross-tail current of the sheet when a southward IMF is present more than doubles compared to the case when no IMF is present.

In Figure 7 the magnitude and shape of the cross tail current on the meridian

cross section of the magnetotail plasma sheet is shown as a function of color for three of the simulations. Magnetic field lines are also drawn. Four different times reveal the progressive changes as reconnection begins to occur when a southward IMF or no IMF is present. From this, we see that reconnection occurs where the cross-tail current peaks which follows directly from equations 3 and 5. It is this current which triggers diffusion and reconnection of the magnetic field and is not the result of spontaneous tearing instability as argued in many places[e.g., *Wang et al.*, 1990, *Liu*, 1991]. Why does the current peak at about $15R_E$? It is here that the magnetic pressure from Earth's dipole field balances the plasma sheet pressure which is exerted by the solar wind [also see *Kageyama et al.*, 1991, *Tsyganenko*, 1998, *Erickson*, 1984]. This region becomes the boundary between the hard inner core dipole field and the streaming tail field lines. The magnetic field can be easily deformed so the current can therefore flow most freely. And since current triggers reconnection provided there is a finite resistivity, reconnnection processes occur here. For both the cases when a southward IMF is present and no IMF is present, the location of the current peak is the same. This is because, far from the Earth, the magnetic pressure of the dipole field drops off abruptly with the sixth power of distance. The difference between the force exerted by the dynamic pressure of the solar wind and that of a the dynamic pressure complemented by draping, reconnected IMF is not nearly large enough to affect a change in the location where plasma pressure balances that of the dipole field pressure. Additionally, for the same reason, the current peak and reconnection point do not shift more than a few R_E over time.

With this in mind, it does not appear that a change in solar wind speed or pressure would greatly affect the location of plasma sheet reconnection processes, though no simulation was performed to test this hypothesis.

There has been much observational evidence that the location of plasma sheet reconnection is indeed this close to the Earth [e.g., *Kettman et al.*, 1990; *Fritz et al.*, 1984]. Though the question of where the reconnection line is located is far from settled it seems that under the circumstances presented in this simulation, near-Earth reconnection is indeed taking place. It is quite possible that there are different types of magnetosphere substorms.

The magnetotail lobes act as large pistons directed against each other at the plasma sheet with the solar wind pushing the outer ends. When reconnected field lines drape the tail lobes and increase their flux density, the magnetic pressure in-

creases. In addition, the large scale structural changes of the magnetosphere increase the surface area and angle of the magnetopause being exerted upon by the solar wind. Both of these factors increase the force of compression that reaches the plasma sheet.

Due to reconnection in the plasma sheet, plasma is accelerated away from the X-line on both sides. This acceleration is directly proportional to the external driving force. The added force due to the presence of reconnected IMF may be seen by comparing the velocity of tailward plasma sheet flow for the cases simulated. When no IMF is present, the tailward velocity of plasma on the tailside of the reconnection X line at the Sun-Earth axis due to this acceleration approaches its peak at about $x = -30R_E$ of about $1.3 \times 10^5\ km/s$ or about 50% of the solar wind speed (see Figure 8-D and Figure 6-II). When a southward IMF is present, the speed at the same location reaches its maximum of about $2.1 \times 10^5\ km/s$ or about 70% of the solar wind speed and several times faster than the local Alfvén speed. The sunward flow dayside of the reconnection point is also faster for the case when a southward IMF is present as compared to the case when no IMF is present.

Satellite Observations of a slow shock layer sandwiching the plasma sheet and accelerated plasma flow have been reported[see *Liu*, 1987 for a review]. This shock region is thought to be extremely thin, $\approx 1000kms$. The grid spacing of this simulation in the near Earth plasma sheet, however, is about $3000kms$. Therefore, it is not surprising that even though plasma flow in the tail is super-Alfvénic, a shock, i.e., Rangkine-Heugonot jump conditions are not completely satisfied and, for the same reason, field aligned currents are not clearly observed. Because the cross-tail current is not redirected along magnetic field lines mapping down to the ionosphere, the large inductance of the magnetosphere prevents a current disruption.

Reconnection in the plasma sheet leads to the expansion and ejection of a large magnetic island on the order of $80R_E$ in diameter. The plasmoid takes tailward hot plasma from the sheet which would produce some of the same effects as the convection surges and rarefaction waves described by Liu[1991]. Even in the absence of an IMF such a structure does develop. However, its development and ejection speed is slow. In the presence of a southward IMF, the plasmoid expansion rate and acceleration increase. However, it's final speed does not greatly exceed the speed of ejection when no IMF was present. The position of the plasmoid O point is plotted as a function of time in Figure 10. From this we can see that explosive reconnection processes under the influence of a southward IMF leads to an initial,

explosive acceleration of the plasmoid after which its velocity becomes a constant of about $\approx 100km/s$. This agrees well with ideas on the early, expansion stage of plasmoid development. However, based on satellite observations, measurements of plasmoid-like structures seem to reveal that they can accelerate to $1000km/s$. The fact that these simulation results did not show this secondary acceleration may indicate that such acceleration cannot be explained with the current model or that the simulation region is still too small. This is still unclear. A closer look at Figure 2-A reveals that as dayside reconnection progresses, the magnetosphere gets fatter. Solar wind flow is diverted out of the simulation region. Note that the simulation was performed in a larger region than drawn. Nevertheless, the plasma flow does get diverted out of the simulation box. Therefore, the solar wind dynamic pressure and the reconnected IMF do not exert a realistic force on the magnetopause. This is because the simulation region is too small in the z axis direction. In the real magnetosphere, the draping reconnected field lines and solar wind flow should exert an even larger force on the lobes than produced here. Tailward boundary effects may also contribute to the slow plasmoid ejection speed.

The 3-D structure of the plasmoid is altered due to the increased compression of a southward IMF. When no IMF was present, plasma sheet reconnection was patchy, leading to several small, intertwined clumps of plasmoids that became quite round under the tension of magnetic field lines [*Kageyama et al.*,1991]. However, in the presence of a southward IMF, plasma sheet reconnection was cleaner, leading to the development of one large plasmoid that was squeezed into a ellispoid, tear drop shape.

Now we turn to a phenomenon not previously observed in simulation results, though expected theoretically. Should a southward IMF continuously impede the magnetosphere, dayside magnetic erosion would lead to the disappearance of the dayside magnetosphere. However, magnetic flux from the tail is brought in to replace the dayside magnetic flux. This is accomplished when plasma flowing from the tail to the dayside within the magnetosphere brings magnetic flux with it. The flow of flux from the tail to the dayside portion of the magnetosphere is controlled by the magnetic presure gradient and by the sunward acceleration of plasma in the plasma sheet. This flow can be seen clearly in Figure 8-A which depicts the equatorial cross section of plasma flow velocity vectors and magnetic neutral lines. This is the Region 1 vortex flow.

Another result of this simulation is that a northward IMF serves as an 'off-switch' of plasma sheet reconnection processes. As described above, reconnecting northward IMF lines strip magnetic flux away from the lobes, thus decreasing the forces which compress the plasma sheet. Figure 6-I shows that the pressure drops and the cross tail current becomes insignificant. For this reason, plasma sheet reconnection is completely inhibited. Figure 3 and Figure 7 further reveal the extent to which the plasma sheet has been decompressed. In addition, reconnecting northward IMF field lines collect on the magnetosphere surface, thus extending the distance of the dayside magnetopause sunward, at $t = 2.5hours$, to $x \approx 15R_E$. This may reflect the fact that the reconnection rate of the simulation was too fast compared with the actual one, so that the collected flux on the dayside could not be swiftly removed from the dayside to the nightside.

For the case when a southward IMF was replaced with a northward IMF, plasma sheet reconnection processes were significantly inhibited. As before, we examine Figure 6-I which shows clearly why reconnection processes in the plasma sheet were inhibited. The cross tail current was damped under the effects of a northward IMF. In addition, the ejection of the plasmoid is slowed slightly as can be seen in Figure 10. From this, we may conclude that the explosive reconnection processes in the plasma sheet can not only be turned on by a southward IMF, but they may also tend to be inhibited by a northward IMF.

Conclusions

A southward IMF, upon reconnection along the equatorial plane of the dayside magnetopause does indeed serve as an 'on switch' for explosive plasma sheet reconnection by enhancing the cross-tail current. This leads to the swift formation and ejection of large plasmoids in the magnetotail. Due to plasma sheet reconnection, plasma is accelerated both tailward and towards the Earth, leading to the transport of magnetic flux from the enhanced tail region to the eroded dayside magnetosphere. The reconnection rate and plasmoid formation speed is far greater than for case when no IMF is present, though the location of reconnection processes is about $15R_E$ for both cases.

A northward IMF serves as an 'off switch' of plasma sheet reconnection even if reconnection processes are under way substantially. Due to reconnection along the

cusp shoulder, magnetic flux is pealed away from the outer lobes of the magnetosphere. This inhibits reconnection processes in the plasma sheet by decreasing the cross-tail current. When the magnetosphere is continuously exposed to a northward IMF and the reconnection rate is high, its shape changes dramatically. In order to accomadate a balance of magnetic to dynamic pressure along the magnetopause, the magnetosphere changes its shape from its usual comet-like tail to that ressembling a tadpole as it attempts to return to its dipolar shape.

Acknowledgements

The authors would like to express their sincere gratitude to Professor K. Nishikawa for his continued support and to the Japanese Ministry of Education for funding this work.

References

1. Axford, W.I., Magnetic Field Reconnection, **Magnetic Reconnection in Space and Laboratory Plasmas**, ed. Hones, E.W., Jr., American Geophysical Union, Washington, D.C., 1984.

2. Baker, D.N., Zwickl, R.D., Bame, S.J., Hones, E.W.Jr., Tsurutani, B.T. and Smith, E.J., An ISEE 3 High Time Resolution Study of Interplanetary Parameter Correlations With Magnetospheric Activity *J. Geophys. Res.*, 88, 6230-6242, 1983.

   The Johns Hopkins University Press, Baltimore, 1987.

3. Coroniti, F.V., MHD Aspects of Magnetotail Dynamics, **Magnetotail Physics**, ed. Lui, A.T.Y, pp. 175-181, The Johns Hopkins University Press, Baltimore, 1987.

4. Dungey, J.W., *Cosmic Electrodynamics*, Cambridge University Press, London, 1958.

5. Erickson, G.M., On the Cause of X-Line Formation in the Near-Earth Plasma Sheet, **Magnetic Reconnection**, ed. Hones, E.W., Jr., pp 296-302, American Geophysical Union, Washington, D.C., 1984.

6. Fritz, T.A., Baker, D.N., McPherron, R.L., and Lennartsson, W., Implications of the 1100 UT March 22, 1979, CDAW 6 Substorm Event for the Role of Magnetic Reconnection in the Geomagnetic Tail, **Magnetic Reconnection**, ed. Hones, E.W., Jr., pp 203-206, American Geophysical Union, Washington, D.C., 1984.

7. Hasegawa, A. and Sato, T., **Space Plasma Physics, 1. Staionary Processes**, Springer-Verlag, New York, 1989.

8. Hautz, R. and Scholer, M., Numerical Simulations on the Structure of Plasmoids in the Deep Tail *Geophys. Res. Letters*, 14, 969-972, 1987.

9. Hones, E.W. Jr., Birn, J., Bame, S.J., Paschmann, G., and Russell, T., On the Three-Dimensional Structure of the Plasmoid Created in the Magnetotail at Substorm Onset *Geophys. Res. Letters*, 9, 203-206, 1982.

10. Hones, E.W. Jr. and Schindler, K., Magnetotail Plasma Flow During Substorms: A Survey with IMP 6 and IMP 8 Satellites, *J. Geophys. Res.*, 84, 7155, 1979.

11. Kageyama, A., Watanabe, K and Sato, T, Global Simulation of the Magnetosphere with a Long Tail:No IMF, submitted for publication to *J. Geophys. Res.*, 1990.

12. Kettmann, G., Fritz, T.A., and Hones, E.W.Jr., Further Evidence for the Creation of a Near-Earth Substorm Neutral Line: CDAW 7 Revisited, *J. Geophys. Res.*, 95, 12045, 1990.

13. Lui, A.T.Y., Observations on the Fluid Aspects of Magnetotail Dynamics, **Magnetotail Physics**, ed. Lui, A.T.Y,pp. 101-118, The Johns Hopkins University Press, Baltimore, 1987.

14. Lui, A.T.Y., A Synthesis of Magnetospheric Substorm Models, *J. Geophys. Res.*, 96, 1849-1856, 1991.

15. Richardson, I.G., Owen, C.J., Cowley, S.W.H., Galvin, A.B., Sanderson, T.R., Scholer, M., Slavin, J.A., and Zwickl, R.D., ISEE 3 Observations During the CDAW 8 Intervals: Case Studies of the Distant Geomagnetic Tail Covering a Wide Range of Geomagnetic Activity, *J. Geophys. Res.*, 94, 15189-15220, 1989.

16. Rostoker, G., Triggering of Expansive Phase Intensifications of Magneticspheric Substorms by Northward Turnings of the Interplanetary Magnetic Field, *J. Geophys. Res.*, 88, 6981-6993, 1983.

17. Shi, Y., Wu, C.C., and Lee, L.C., A Study of Multiple X Line Reconnection at the Dayside Magnetopause *Geophys. Res. Letters*, 15, 4, 295-298, 1982.

18. Slavin, J.A., Baker, D.N., Craven, J.D., Elphic, R.C., Fairfield, D.H., Frank, L.A., Galvin, A.B., Hughes, W.J., Manka, R.H., Mitchell, D.G., Richardson, I.G., Sanderson, T.R., Sibeck, D.J., Smith, E.J., and Zwickl, R.D., CDAW 8 Observations of

Plasmoid Signatures in the Geomagnetic Tail: An Assessment, *J. Geophys. Res.*, 94, 15153, 1989.

19. Sato, T., Strong Plasma Acceleration by Slow Shocks Resulting from Magnetic Reconnection, *J. Geophys. Res.*, 84, 7177, 1979.

20. Sato, T. and Hayashi, T., Externally Driven Magnetic Reconnection and a Powerful Magnetic Energy Converter, *Phys. Fluids*, 22(6), 1189, 1979.

21. Sato, T., Walker, Raymond J., and Ashour-Abdalla, M., Driven Magnetic Reconnection in Three Dimensions: Energy Conversion and Field Aligned Current Generation, *J. Geophys. Res.*, 89, 9761-9769, 1984.

22. Sauvard, J.A. et al, A Case Study of the Large Scale Response of the Magnetosphere to a Southward Turning of the IMF, **Magnetotail Physics**, ed. Lui, A.T.Y,pp. 143-154, The Johns Hopkins University Press, Baltimore, 1987.

23. Tsyganenko, N.A., On the Re-Distribution of the Magnetic Field and Plasma in the Near Nightside Magnetosphere During a Substorm Growth Phase, *Planet. Space Sci.*, 37, 183-192, 1989.

24. Watanabe, K., Ashour-Abdalla, M., and Sato, T., A Numerical Model of Magnetosphere-Ionosphere Coupling: Preliminary Results, *J. Geophys. Res.*, 91, 6973-6978, 1986.

25. Watanabe, K. and Sato, T., Global Simulation of the Solar Wind-Magnetosphere interaction: The Importance of Its Numerical Validity, *J. Geophys. Res.*, 95, 75, 1990.

26. Zanetti, L.J., Potemra, T.A., Erlandson, R.E., Bythrow, P.F., Anderson, B.J., Murphree, J.S., and Markland, G.T., Polar Region Birkland Current, Convection, and Aurora for Northward Interplanetary Magnetic Field, *J. Geophys. Res.*, 95, 5825-5833, 1990.

Figure Captions

Figure 1: A)Current vectors drawn on the equatorial cross section just after the formation of the magnetosphere at t=1hour after the start of the simulation. An IMF has not yet been introduced. B)Pressure($kg/m \cdot s^2$), temperature(kev), and cross-tail current($nAmp/m^3$) along the x axis.

Figure 2: Equatorial and meridian cross-sections showing the plasma flow lines and magnetic field lines over a 1.5 hour period for the case when a southward IMF is present in the solar wind. Due to reconnection in the plasma sheet, a plasmoid develops and is accelerated towards the tail boundary.

Figure 3: Equatorial and meridian cross-sections showing the plasma flow lines and magnetic field lines over a 1.5hour period for the case when a northward IMF is present in the solar wind. Reconnection along the shoulder cusp strips magnetotail lobe flux away, thus decreasing the magnetic pressure exerted along the magnetopause.

Figure 4: Structure of the magnetosphere for the case when a southward IMF is present for one hour(from A-B), then a northward IMF is introduced(from B-C).

Figure 5: Values at $t \approx 2.1 hours$ of plasma pressure($kg/m \cdot s^2$), temperature(kev), log B, and cross tail current, Cy($nAmp/m^3$), along the x-axis when the solar wind contains A)A southward IMF B)A northward IMF C)southward→northward IMF D)no IMF.

Figure 6: I-Variation over time of plasma pressure($kg/m \cdot s^2$), temperature(kev), and cross-tail current($nAmp/m^3$) in the plasma sheet at about 14 earth radii behind the earth when the solar wind contains A)a southward IMF, B)a northward IMF, C)a southward then northward IMF, D)no IMF. II-Variation over time of tailward plasma velocity at about 30 earth radii behind the earth for the same.

Figure 7: Cross section showing the magnitude of the cross-tail current as a function of color and line structure of the geomagnetic field(green), plasmoid(yellow), and IMF(Red) in the plasma sheet for four times when A)a southward IMF, B)no IMF, C)a northward IMF is present. The region shown is defined over $-10R_E \leq z \leq 10R_E$ and $-80R_E \leq x \leq 0R_E$. The current peak is clearly the location of sheet reconnection.

Figure 8: Plasma flow velocity vectors and magnetically neutral lines drawn on the equatorial plane for the case when A) a southward IMF, C) no IMF is present. Notice the flow of plasma from the tail towards the dayside magnetosphere in A). This flow brings replacement magnetic flux from the enhanced tail to the eroded dayside region. B)The values of the tailward velocity, V_x and the z component of B over the Sun-Earth axis at times corresponding to figure A). D) same as B) when no IMF is present.

Figure 9: A)Plasma flow velocity vectors and magnetically neutral lines drawn on the equatorial plane for the case when a southward IMF is present for 1 hour and is then changed to a northward IMF and the values of the tailward velocity and B_z over the Sun-Earth axis at $t = 3hours$. B)Plasma vectors when a northward IMF only has been present.

Figure 10: Position in Earth Radii of the plasmoid O-point plotted as a function of time when the solar wind contains A)a southward IMF B)southward→northward IMF C)no IMF.

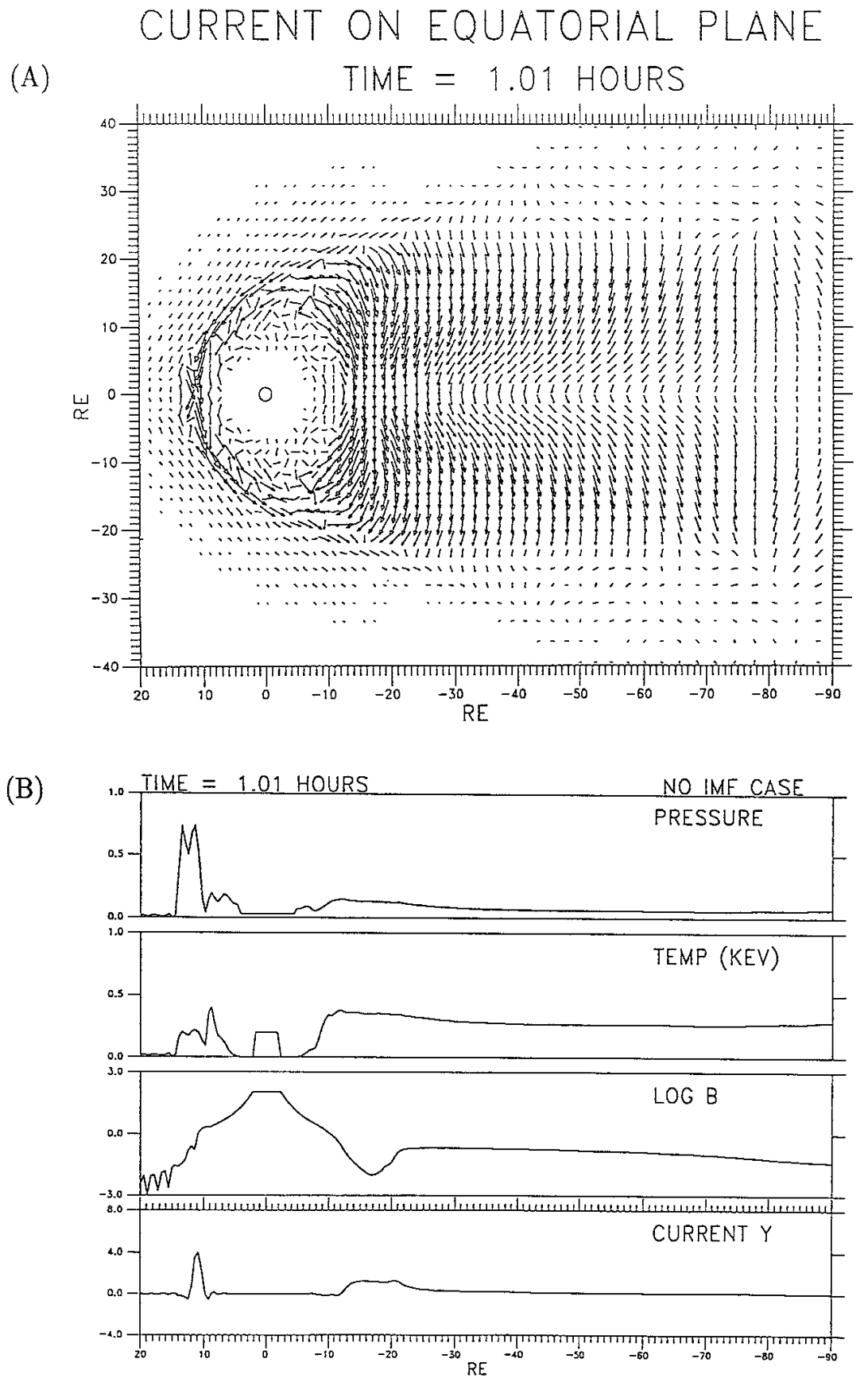
CURRENT ON EQUATORIAL PLANE
(A)
TIME = 1.01 HOURS
RE
RE
(B)
TIME = 1.01 HOURS
NO IMF CASE
PRESSURE
TEMP (KEV)
LOG B
CURRENT Y
RE

Figure 1

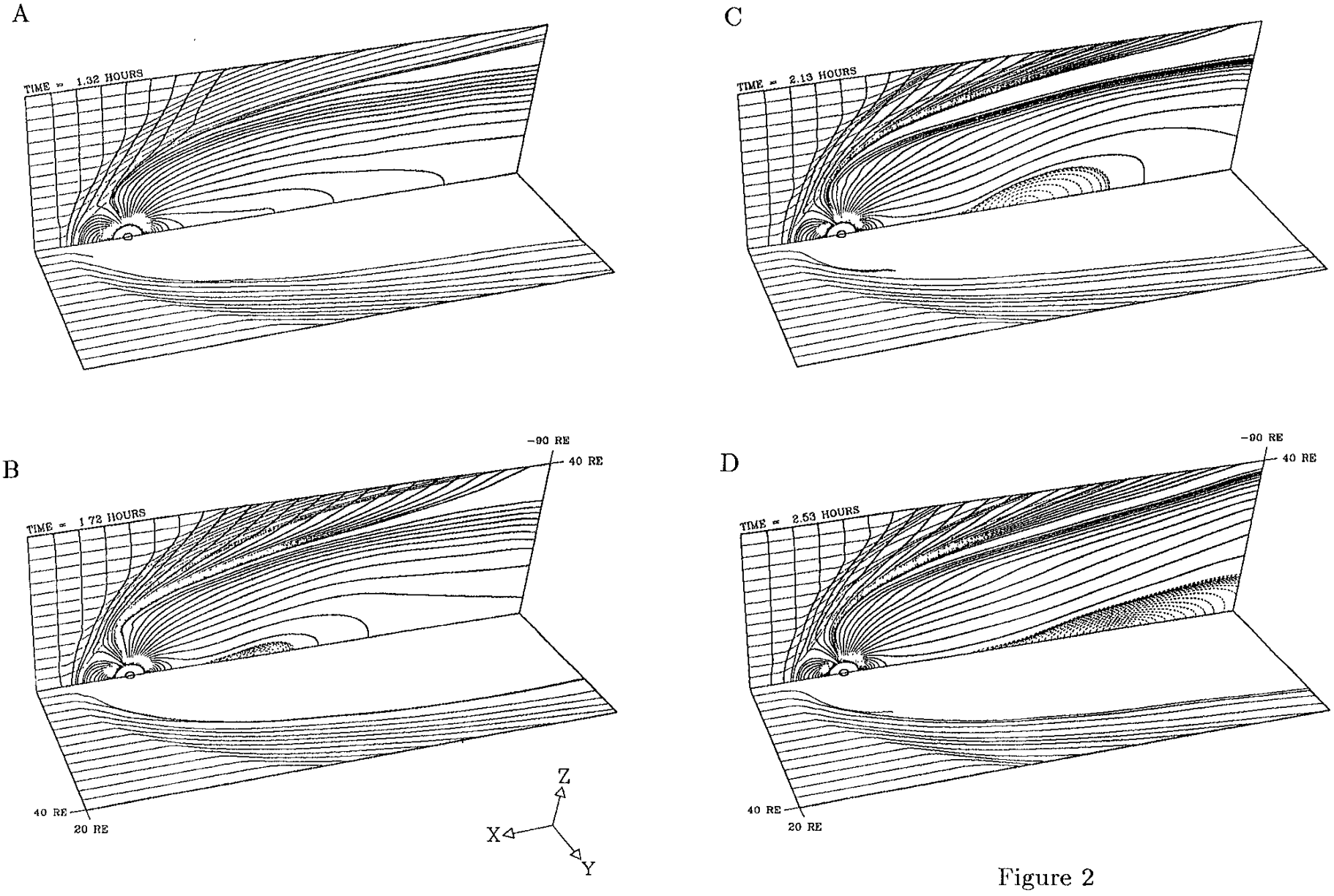
A
TIME = 1.32 HOURS
C
TIME = 2.13 HOURS
B
TIME = 1.72 HOURS
-90 RE
40 RE
40 RE
20 RE
Z
X
Y
D
TIME = 2.53 HOURS
-90 RE
40 RE
40 RE
20 RE

Figure 2

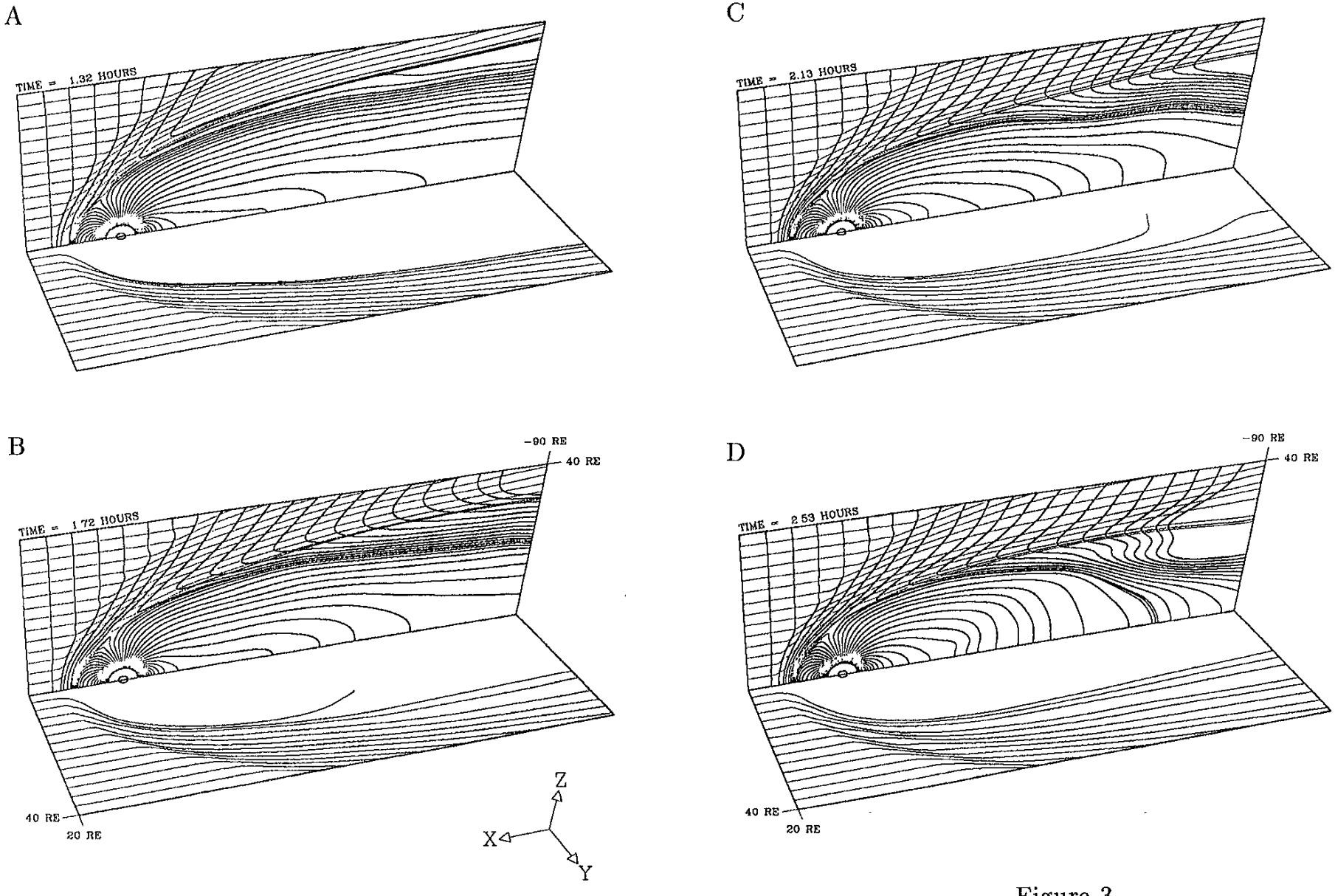
A
TIME = 1.32 HOURS
C
TIME = 2.13 HOURS
B
TIME = 1.72 HOURS
-90 RE
40 RE
40 RE
20 RE
Z
X
Y
D
TIME = 2.53 HOURS
-90 RE
40 RE
40 RE
20 RE

Figure 3

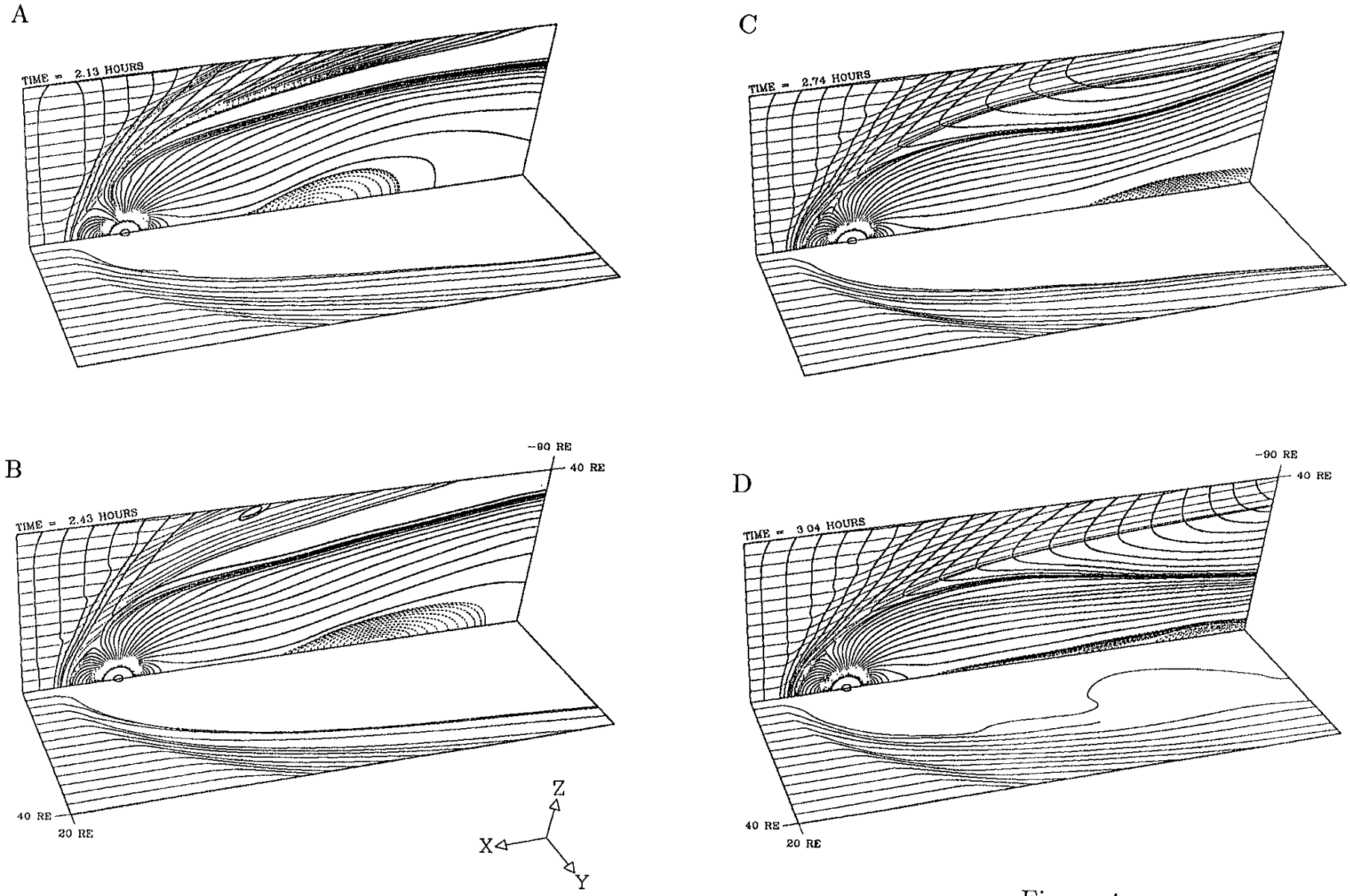
A
TIME = 2.13 HOURS
C
TIME = 2.74 HOURS
B
TIME = 2.43 HOURS
-90 RE
40 RE
40 RE
20 RE
Z
X
Y
D
TIME = 3.04 HOURS
-90 RE
40 RE
40 RE
20 RE

Figure 4

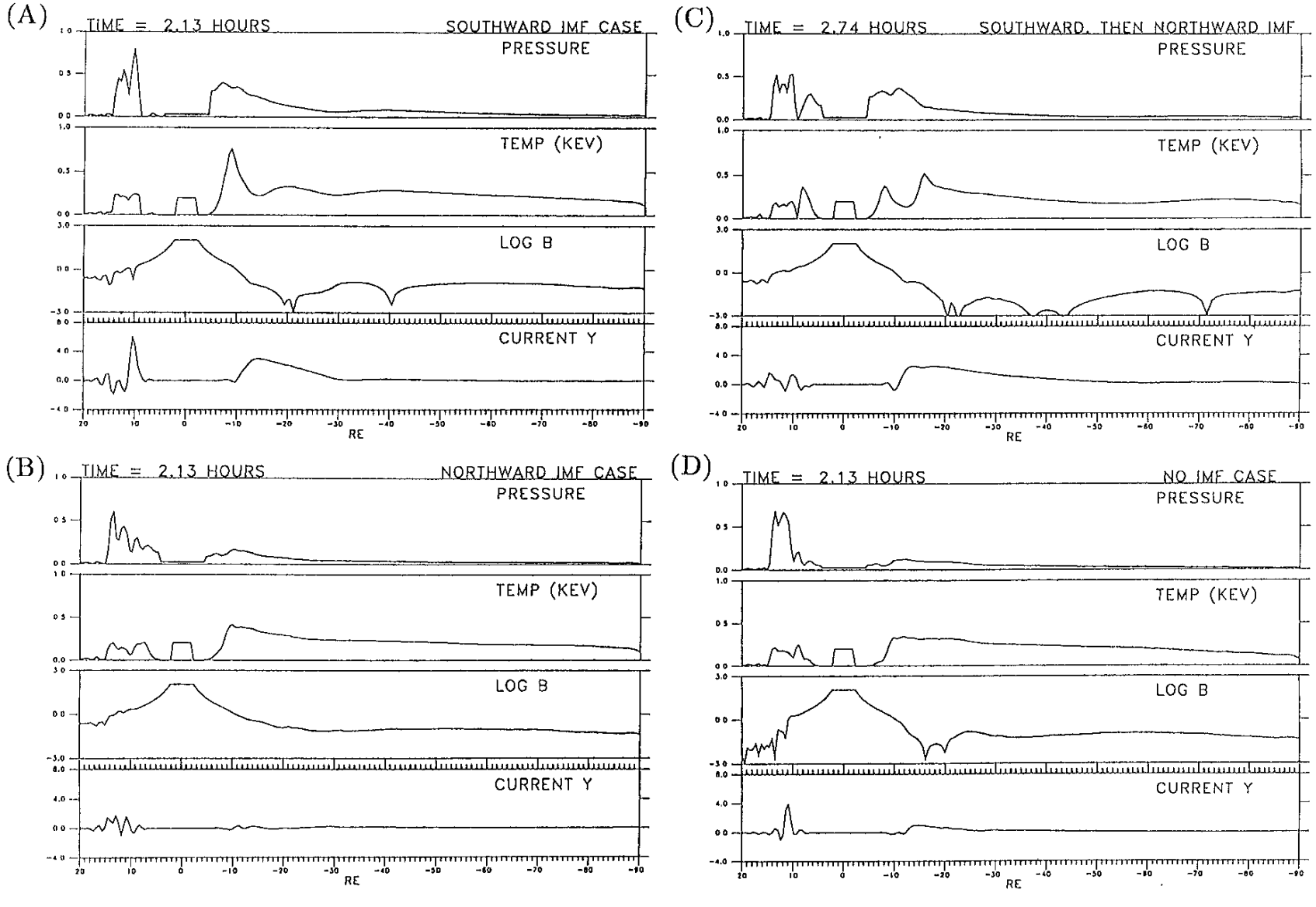
(A)
TIME = 2.13 HOURS
SOUTHWARD IMF CASE
PRESSURE
TEMP (KEV)
LOG B
CURRENT Y
RE
(B)
TIME = 2.13 HOURS
NORTHWARD IMF CASE
PRESSURE
TEMP (KEV)
LOG B
CURRENT Y
RE
(C)
TIME = 2.74 HOURS
SOUTHWARD, THEN NORTHWARD IMF
PRESSURE
TEMP (KEV)
LOG B
CURRENT Y
RE
(D)
TIME = 2.13 HOURS
NO IMF CASE
PRESSURE
TEMP (KEV)
LOG B
CURRENT Y
RE

Figure 5

6-I

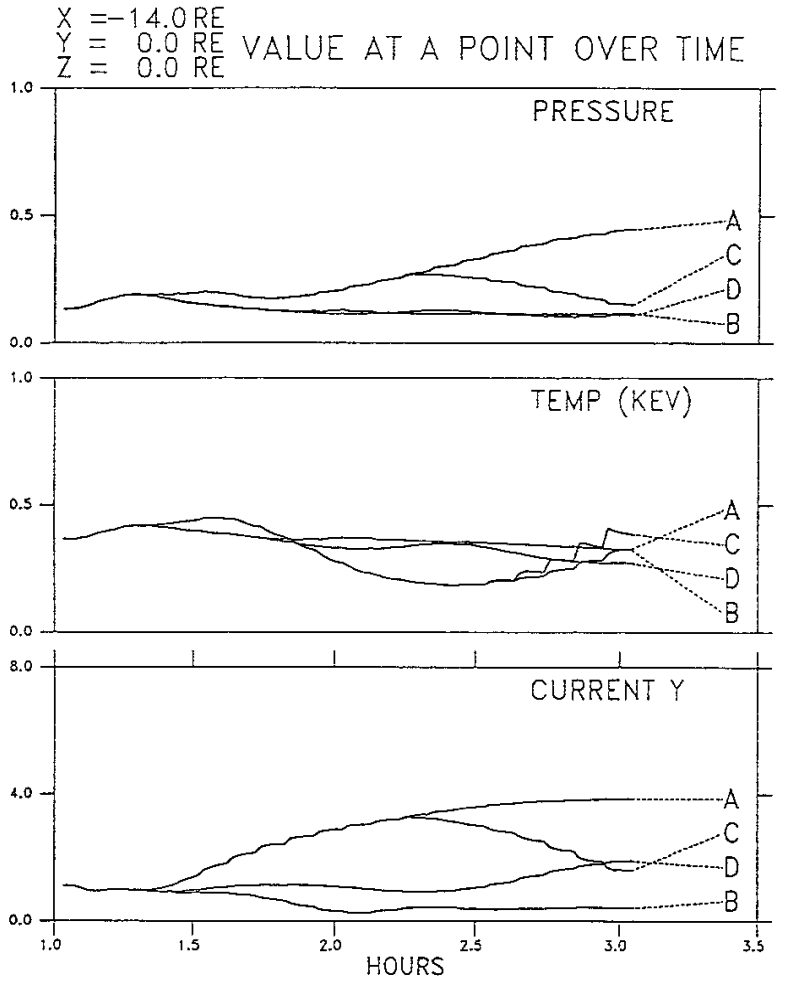

6-II

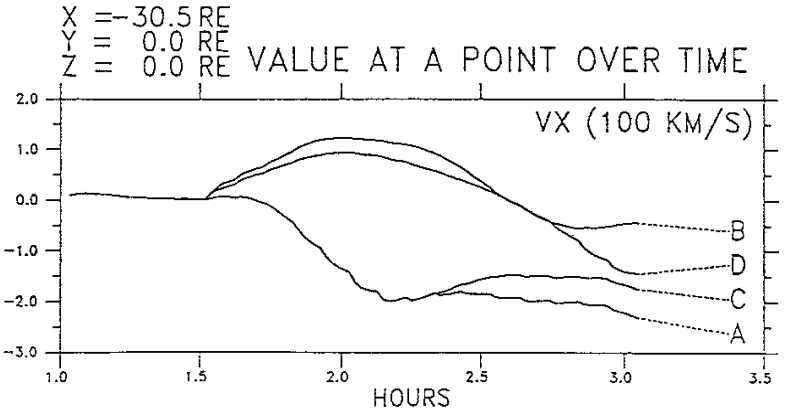

Figure 6

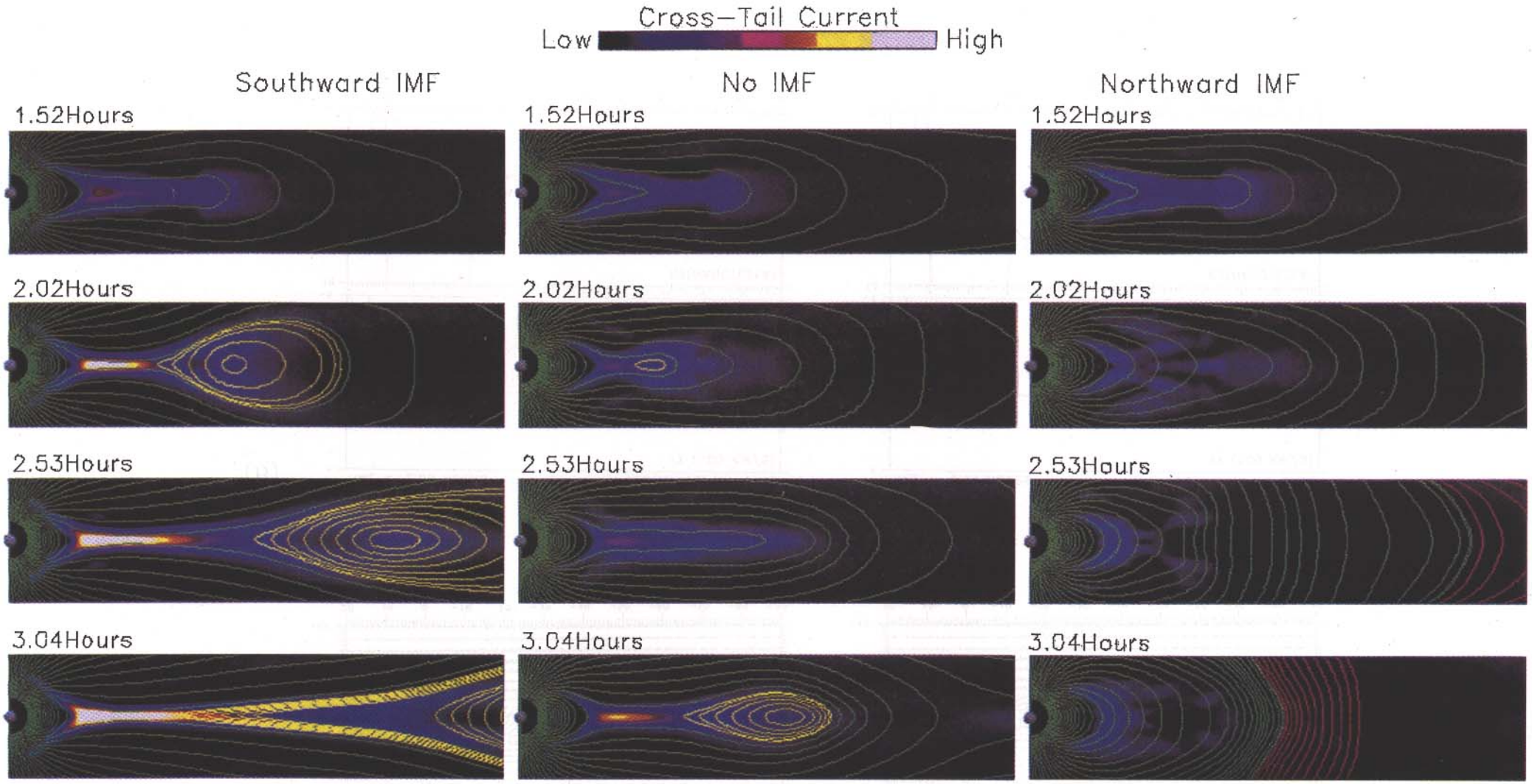
Cross–Tail Current
Low
High
Southward IMF
No IMF
Northward IMF
1.52Hours
2.02Hours
2.53Hours
3.04Hours
1.52Hours
2.02Hours
2.53Hours
3.04Hours
1.52Hours
2.02Hours
2.53Hours
3.04Hours
(A)
(B)
(C)

Figure 7

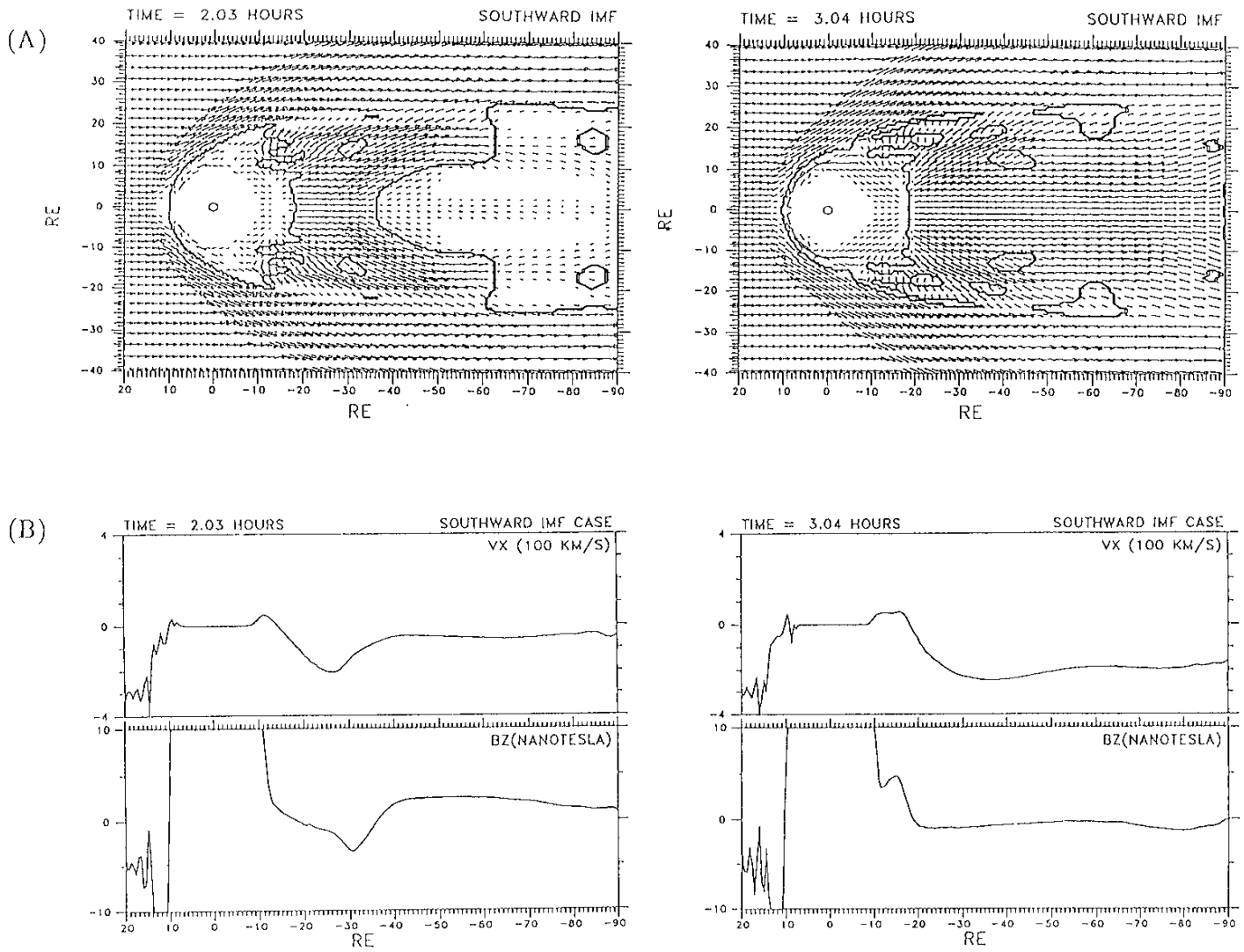
(A)
TIME = 2.03 HOURS
SOUTHWARD IMF
TIME = 3.04 HOURS
SOUTHWARD IMF
RE
RE
(B)
TIME = 2.03 HOURS
SOUTHWARD IMF CASE
VX (100 KM/S)
BZ(NANOTESLA)
TIME = 3.04 HOURS
SOUTHWARD IMF CASE
VX (100 KM/S)
BZ(NANOTESLA)
RE
RE

Figure 8

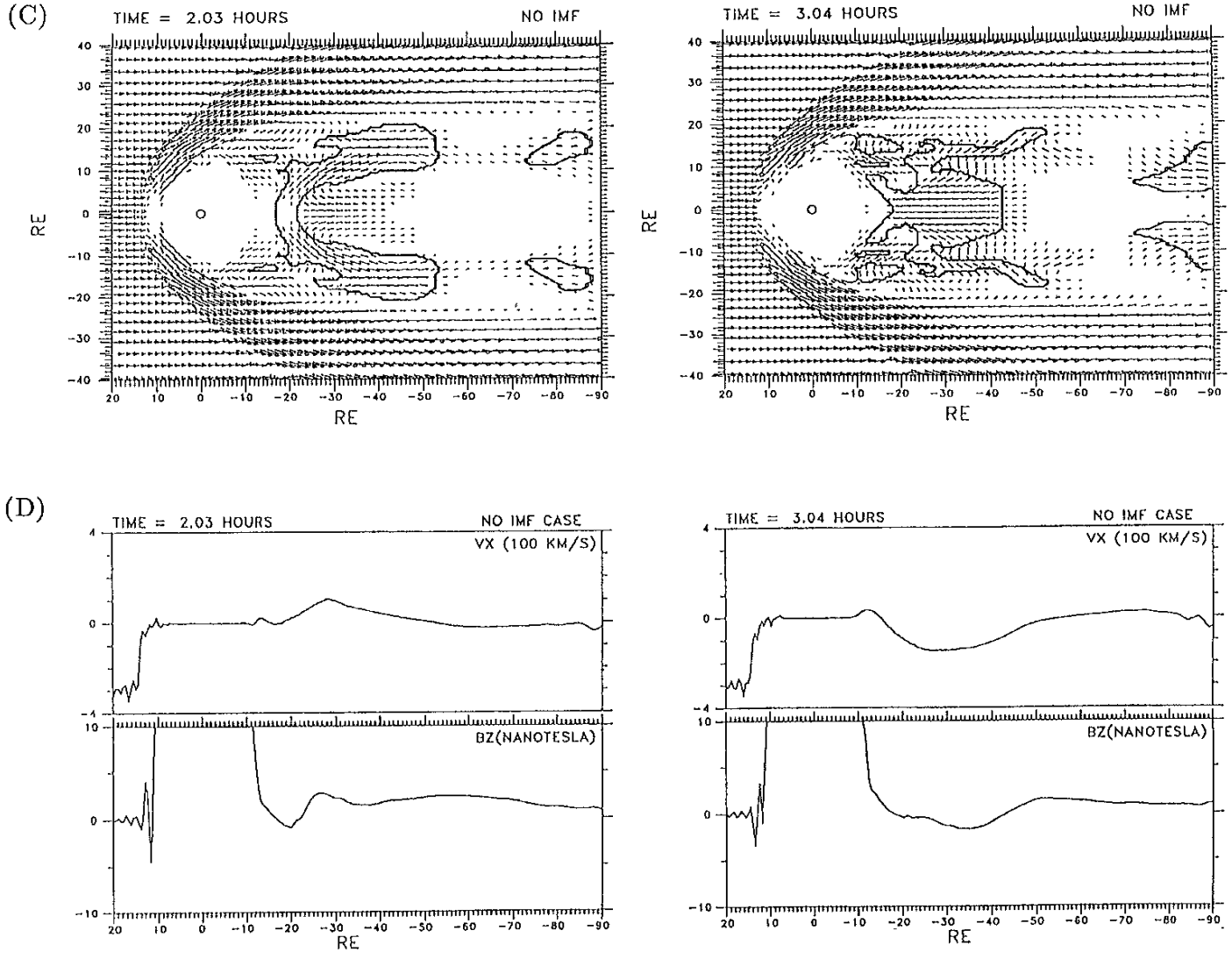

Figure 8: continued.

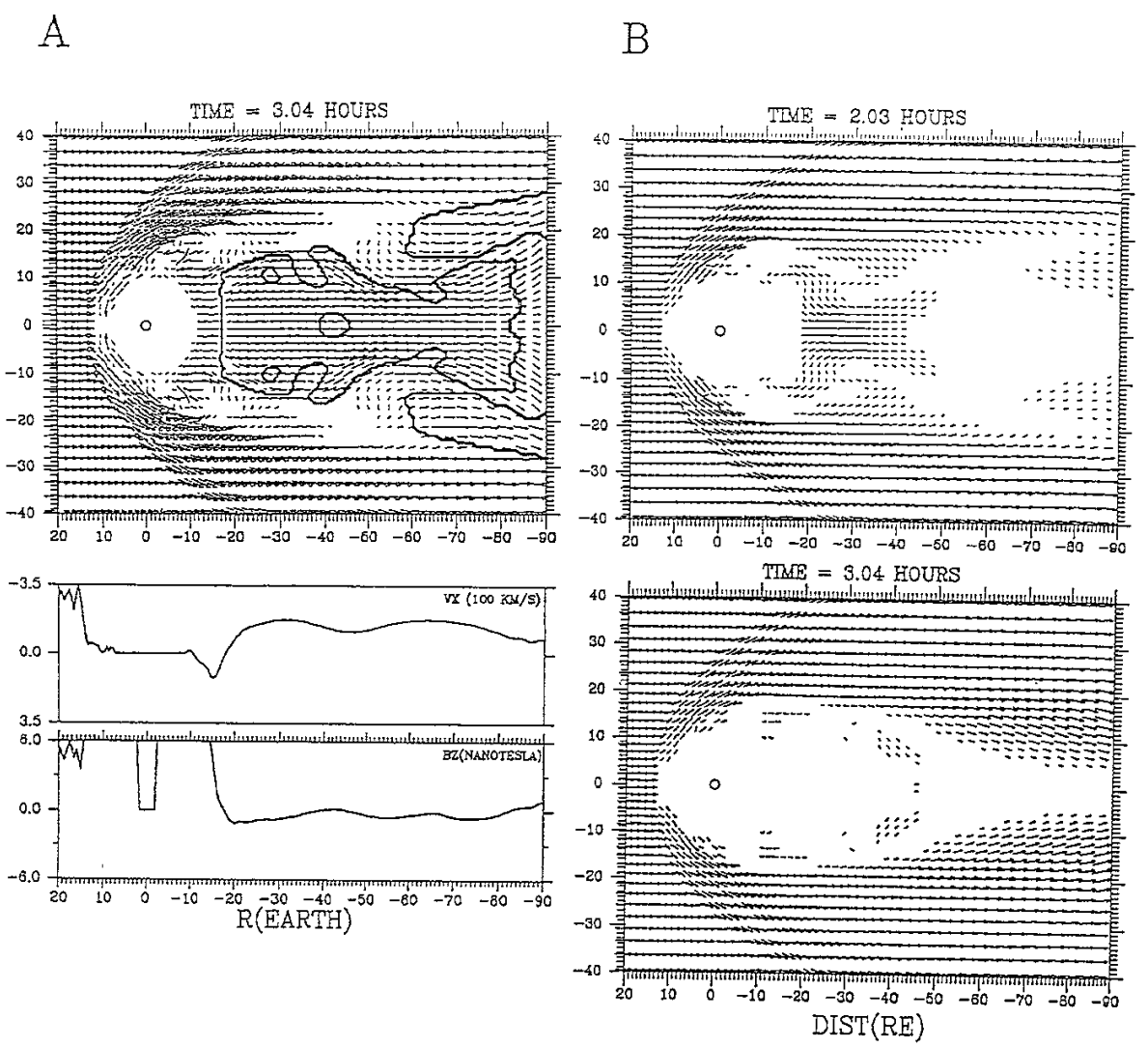
A
B
TIME = 3.04 HOURS
TIME = 2.03 HOURS
TIME = 3.04 HOURS
VX (100 KM/S)
BZ(NANOTESLA)
R(EARTH)
DIST(RE)

Figure 9

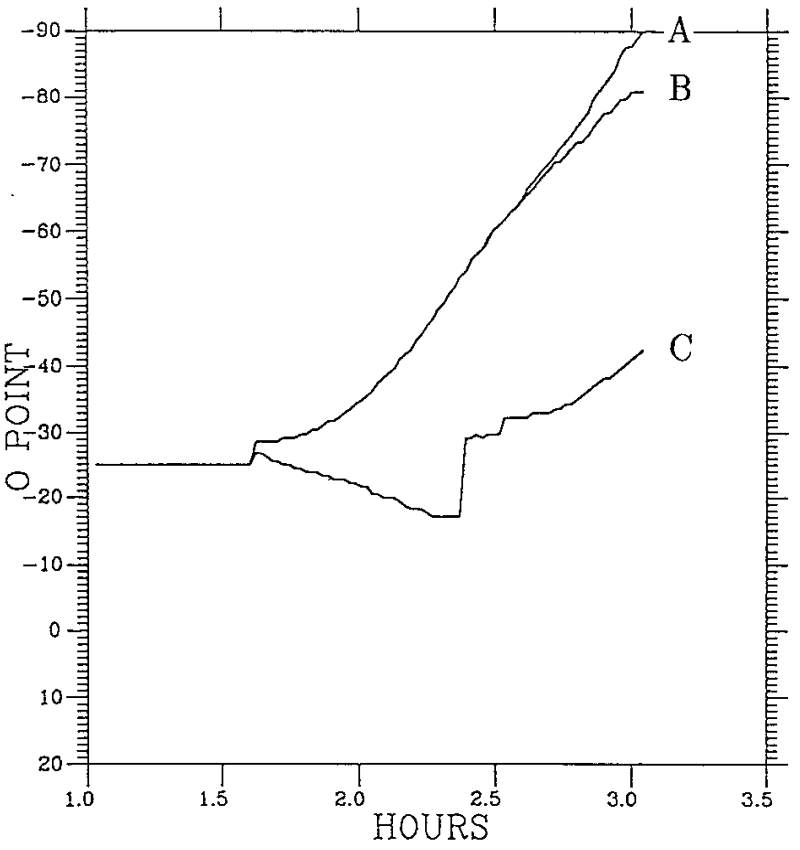
-90
-80
-70
-60
-50
-40
-30
-20
-10
0
10
20
DEW POINT
1.0
1.5
2.0
2.5
3.0
3.5
HOURS
A
B
C

Figure 10

Recent Issues of NIFS Series

NIFS-43 K.Yamazaki, N.Ohyabu, M.Okamoto, T.Amano, J.Todoroki, Y.Ogawa, N.Nakajima, H.Akao, M.Asao, J.Fujita, Y.Hamada, T.Hayashi, T.Kamimura, H.Kaneko, T.Kuroda, S.Morimoto, N.Noda, T.Obiki, H.Sanuki, T.Sato, T.Satow, M.Wakatani, T.Watanabe, J.Yamamoto, O.Motojima, M.Fujiwara, A.Iiyoshi and LHD Design Group, *Physics Studies on Helical Confinement Configurations with l=2 Continuous Coil Systems*; Sep. 1990

NIFS-44 T.Hayashi, A.Takei, N.Ohyabu, T.Sato, M.Wakatani, H.Sugama, M.Yagi, K.Watanabe, B.G.Hong and W.Horton, *Equilibrium Beta Limit and Anomalous Transport Studies of Helical Systems*; Sep. 1990

NIFS-45 R.Horiuchi, T.Sato, and M.Tanaka, *Three-Dimensional Particle Simulation Study on Stabilization of the FRC Tilting Instability*; Sep. 1990

NIFS-46 K.Kusano, T.Tamano and T. Sato, *Simulation Study of Nonlinear Dynamics in Reversed-Field Pinch Configuration*; Sep. 1990

NIFS-47 Yoshi H.Ichikawa, *Solitons and Chaos in Plasma*; Sep. 1990

NIFS-48 T.Seki, R.Kumazawa, Y.Takase, A.Fukuyama, T.Watari, A.Ando, Y.Oka, O.Kaneko, K.Adati, R.Akiyama, R.Ando, T.Aoki, Y.Hamada, S.Hidekuma, S.Hirokura, K.Ida, K.Itoh, S.-I.Itoh, E.Kako, A. Karita, K.Kawahata, T.Kawamoto, Y.Kawasumi, S.Kitagawa, Y.Kitoh, M.Kojima, T.Kuroda, K.Masai, S.Morita, K.Narihara, Y.Ogawa, K.Ohkubo, S.Okajima, T.Ozaki, M.Sakamoto, M.Sasao, K.Sato, K.N.Sato, F.Shinbo, H.Takahashi, S.Tanahashi, Y.Taniguchi, K.Toi and T.Tsuzuki, *Application of Intermediate Frequency Range Fast Wave to JIPP T-IIU Plasma*; Sep.1990

NIFS-49 A.Kageyama, K.Watanabe and T.Sato, *Global Simulation of the Magnetosphere with a Long Tail: The Formation and Ejection of Plasmoids*; Sep.1990

NIFS-50 S.Koide, *3-Dimensional Simulation of Dynamo Effect of Reversed Field Pinch*; Sep. 1990

NIFS-51 O.Motojima, K. Akaishi, M.Asao, K.Fujii, J.Fujita, T.Hino, Y.Hamada, H.Kaneko, S.Kitagawa, Y.Kubota, T.Kuroda, T.Mito, S.Morimoto, N.Noda, Y.Ogawa, I.Ohtake, N.Ohyabu, A.Sagara, T. Satow, K.Takahata, M.Takeo, S.Tanahashi, T.Tsuzuki, S.Yamada, J.Yamamoto, K.Yamazaki, N.Yanagi, H.Yonezu, M.Fujiwara, A.Iiyoshi and LHD Design Group, *Engineering Design Study of Superconducting Large Helical Device*; Sep. 1990

NIFS-52 T.Sato, R.Horiuchi, K. Watanabe, T. Hayashi and K.Kusano, *Self-Organizing Magnetohydrodynamic Plasma*; Sep. 1990

NIFS-53 M.Okamoto and N.Nakajima, *Bootstrap Currents in Stellarators and Tokamaks*; Sep. 1990

NIFS-54 K.Itoh and S.-I.Itoh, *Peaked-Density Profile Mode and Improved Confinement in Helical Systems*; Oct. 1990

NIFS-55 Y.Ueda, T.Enomoto and H.B.Stewart, *Chaotic Transients and Fractal Structures Governing Coupled Swing Dynamics*; Oct. 1990

NIFS-56 H.B.Stewart and Y.Ueda, *Catastrophes with Indeterminate Outcome*; Oct. 1990

NIFS-57 S.-I.Itoh, H.Maeda and Y.Miura, *Improved Modes and the Evaluation of Confinement Improvement*; Oct. 1990

NIFS-58 H.Maeda and S.-I.Itoh, *The Significance of Medium- or Small-size Devices in Fusion Research*; Oct. 1990

NIFS-59 A.Fukuyama, S.-I.Itoh, K.Itoh, K.Hamamatsu, V.S.Chan, S.C.Chiu, R.L.Miller and T.Ohkawa, *Nonresonant Current Drive by RF Helicity Injection*; Oct. 1990

NIFS-60 K.Ida, H.Yamada, H.Iguchi, S.Hidekuma, H.Sanuki, K.Yamazaki and CHS Group, *Electric Field Profile of CHS Heliotron/Torsatron Plasma with Tangential Neutral Beam Injection*; Oct. 1990

NIFS-61 T.Yabe and H.Hoshino, *Two- and Three-Dimensional Behavior of Rayleigh-Taylor and Kelvin-Helmholz Instabilities*; Oct. 1990

NIFS-62 H.B. Stewart, *Application of Fixed Point Theory to Chaotic Attractors of Forced Oscillators;* Nov. 1990

NIFS-63 K.Konn., M.Mituhashi, Yoshi H.Ichikawa,*Soliton on Thin Vortex Filament;* Dec. 1990

NIFS-64 K.Itoh, S.-I.Itoh and A.Fukuyama,*Impact of Improved Confinement on Fusion Research;* Dec. 1990

NIFS -65 A.Fukuyama, S.-I.Itoh and K. Itoh,*A Consistency Analysis on the Tokamak Reactor Plasmas;* Dec. 1990

NIFS-66 K.Itoh, H. Sanuki, S.-I. Itoh and K. Tani,*Effect of Radial Electric Field on α-Particle Loss in Tokamaks;* Dec. 1990

NIFS-67 K.Sato,and F.Miyawaki,*Effects of a Nonuniform Open Magnetic Field on the Plasma Presheath*; Jan.1991

NIFS-68 K.Itoh and S.-I.Itoh,*On Relation between Local Transport Coefficient and Global Confinement Scaling Law;* Jan. 1991

NIFS-69 T.Kato, K.Masai, T.Fujimoto,F.Koike, E.Källne, E.S.Marmar and J.E.Rice,*He-like Spectra Through Charge Exchange Processes in Tokamak Plasmas;* Jan.1991

NIFS-70 K. Ida, H. Yamada, H. Iguchi, K. Itoh and CHS Group, *Observation of Parallel Viscosity in the CHS Heliotron/Torsatron* ; Jan.1991

NIFS-71 H. Kaneko, *Spectral Analysis of the Heliotron Field with the Toroidal Harmonic Function in a Study of the Structure of Built-in Divertor* ; Jan. 1991

NIFS-72 S. -I. Itoh, H. Sanuki and K. Itoh, *Effect of Electric Field Inhomogeneities on Drift Wave Instabilities and Anomalous Transport* ; Jan. 1991

NIFS-73 Y.Nomura, Yoshi.H.Ichikawa and W.Horton, *Stabilities of Regular Motion in the Relativistic Standard Map*; Feb. 1991

NIFS-74 T.Yamagishi, *Electrostatic Drift Mode in Toroidal Plasma with Minority Energetic Particles*, Feb. 1991

NIFS-75 T.Yamagishi, *Effect of Energetic Particle Distribution on Bounce Resonance Excitation of the Ideal Ballooning Mode*, Feb. 1991

NIFS-76 T.Hayashi, A.Tadei, N.Ohyabu and T.Sato, *Suppression of Magnetic Surface Breading by Simple Extra Coils in Finite Beta Equilibrium of Helical System;* Feb. 1991

NIFS-77 N. Ohyabu, *High Temperature Divertor Plasma Operation*; Feb. 1991

NIFS-78 K.Kusano, T. Tamano and T. Sato, *Simulation Study of Toroidal Phase-Locking Mechanism in Reversed-Field Pinch Plasma*; Feb. 1991

NIFS-79 K. Nagasaki, K. Itoh and S. -I. Itoh, *Model of Divertor Biasing and Control of Scrape-off Layer and Divertor Plasmas*; Feb. 1991

NIFS-80 K. Nagasaki and K. Itoh, *Decay Process of a Magnetic Island by Forced Reconnection*; Mar. 1991

NIFS-81 K. Takahata, N. Yanagi, T. Mito, J. Yamamoto, O.Motojima and LHDDesign Group, K. Nakamoto, S. Mizukami, K. Kitamura, Y. Wachi, H. Shinohara, K. Yamamoto, M. Shibui, T. Uchida and K. Nakayama, *Design and Fabrication of Forced-Flow Coils as R&D Program for Large Helical Device*; Mar. 1991

NIFS-82 T. Aoki and T. Yabe, *Multi-dimensional Cubic Interpolation for ICF Hydrodynamics Simulation*; Apr. 1991

NIFS-83 K. Ida, S.-I. Itoh, K. Itoh, S. Hidekuma, Y. Miura, H. Kawashima, M. Mori, T. Matsuda, N. Suzuki, H. Tamai, T.Yamauchi and JFT-2M Group, *Density Peaking in the JFT-2M Tokamak Plasma with Counter Neutral Beam Injection* ; May 1991

NIFS-84 A. Iiyoshi, *Development of the Stellarator/Heliotron Research*; May 1991

NIFS-85 Y. Okabe, M. Sasao, H. Yamaoka, M. Wada and J. Fujita, *Dependence of Au^- Production upon the Target Work Function in a Plasma-Sputter-Type Negative Ion Source;* May 1991

NIFS-86 N. Nakajima and M. Okamoto, *Geometrical Effects of the Magnetic Field on the Neoclassical Flow, Current and Rotation in General Toroidal Systems*; May 1991

NIFS-87 S. -I. Itoh, K. Itoh, A. Fukuyama, Y. Miura and JFT-2M Group, *ELMy-H mode as Limit Cycle and Chaotic Oscillations in Tokamak Plasmas;* May 1991

NIFS-88 N.Matsunami and K.Kitoh, *High Resolution Spectroscopy of H^+ Energy Loss in Thin Carbon Film;* May 1991

NIFS-89 H. Sugama, N. Nakajima and M.Wakatani, *Nonlinear Behavior of Multiple-Helicity Resistive Interchange Modes near Marginally Stable States;* May 1991

NIFS-90 H. Hojo and T.Hatori, *Radial Transport Induced by Rotating RF Fields and Breakdown of Intrinsic Ambipolarity in a Magnetic Mirror*; May 1991

NIFS-91 M. Tanaka, S. Murakami, H. Takamaru and T.Sato, *Macroscale Implicit, Electromagnetic Particle Simulation of Inhomogeneous and Magnetized Plasmas in Multi-Dimensions;* May 1991

NIFS-92 S. - I. Itoh, *H-mode Physics, -Experimental Observations and Model Theories-, Lecture Notes, Spring College on Plasma Physics, May 27 - June 21 1991 at International Centre for Theoretical Physics (IAEA UNESCO) Trieste, Italy ;* Jun. 1991

NIFS-93 Y. Miura, K. Itoh, S. - I. Itoh, T. Takizuka, H. Tamai, T. Matsuda, N. Suzuki, M. Mori, H. Maeda and O. Kardaun, *Geometric Dependence of the Scaling Law on the Energy Confinement Time in H-mode Discharges;* Jun. 1991

NIFS-94 H. Sanuki, K. Itoh, K. Ida and S. - I. Itoh, *On Radial Electric Field Structure in CHS Torsatron / Heliotron;* Jun. 1991

NIFS-95 K. Itoh, H. Sanuki and S. - I. Itoh,*Influence of Fast Ion Loss on Radial Electric Field in Wendelstein VII-A Stellarator;* Jun. 1991

NIFS-96 S. - I. Itoh, K. Itoh, A. Fukuyama, *ELMy-H mode as Limit Cycle and Chaotic Oscillations in Tokamak Plasmas;* Jun. 1991

NIFS-97 K. Itoh, S. - I. Itoh, H. Sanuki, A. Fukuyama, *An H-mode-Like Bifurcation in Core Plasma of Stellarators;* Jun. 1991

NIFS-98 H. Hojo, T. Watanabe, M. Inutake, M. Ichimura and S. Miyoshi, *Axial Pressure Profile Effects on Flute Interchange Stability in the Tandem Mirror GAMMA 10;* Jun. 1991